The optimization of bimetallic electrodes' sensitivity using copper nucleation on metallic substrates to detect nitrates in seawater

S. Abed, M. Gibilaro, Pierre Chamelot, A. David, C. Barus, Laurent Massot

The optimization of bimetallic electrodes' sensitivity using copper nucleation on metallic substrates to detect nitrates in seawater

S. Abed [a, b], M. Gibilaro [a], P. Chamelot [a], A. David [c], C. Barus [a, b, *], L. Massot [a]

[a] *Laboratoire de Génie Chimique UMR 5503, Département Procédés Electrochimiques, Université Paul Sabatier, 118 route de Narbonne, 31062 Toulouse Cedex, France*

[b] *Laboratoire d'Etudes en Géophysique et Océanographie Spatiales, UMR 5566, Université de Toulouse , CNRS, CNES, IRD, UPS, 18 Avenue Edouard Belin 31401 Toulouse Cedex 9, France*

[c] *nke instrumentation, 6 rue Gutenberg – ZI Kérandré 56700 Hennebont – France*

Abstract

The aim of this work is to highlight the beneficial impact of the nucleation mode study on controlling the electrodeposition of a metal on a substrate, in order to form high sensitivity bimetallic electrodes. Actually, optimizing the electrodeposition operating conditions allows generating the largest active surface, and so, increasing electrode sensitivity.

For this purpose, the nucleation phenomena and the initial growth of copper nuclei on gold, platinum and stainless steel 316L electrodes were investigated using cyclic voltammetry (CV) and chronoamperometry in aqueous media. The experimental results were compared to theoretical models for the two possible nucleation modes: instantaneous and progressive.

Chronoamperometric results showed that the electrodeposition process involves progressive nucleation for copper on the three substrates, which was confirmed by scanning electron microscopy (SEM).

* Corresponding author. Tel.: +33 5 61 55 64 09
E-mail address : carole.barus@univ-tlse3.fr (C. Barus)

Optimal operating conditions were determined for the preparation of the highest active surface area. Subsequently, copper deposition runs were carried out on the three electrode substrates. The formed bimetallic electrodes were tested for their ability to detect low nitrate concentration in artificial seawater using square wave voltammetry (SWV).

Keywords: Electrocrystallisation; bimetallic electrodes; Chronoamperometry; Progressive nucleation; Square wave voltammetry

1. Introduction

The present work focuses on studying the first instant of copper nuclei formation on the electrode surface. The growth of these nuclei over time is studied in order to determine the optimum operating conditions allowing to yield the highest specific surface area as well as a sensitive and stable bimetallic electrode and to put forward a novel effective electrodeposition process. Factors influencing deposit quality must be considered, principally the potential and the cutoff charge. For this intent, the nucleation phenomena of copper on gold, platinum and stainless steel 316L substrates was investigated using cyclic voltammetry and chronoamperometry. The electrodeposition of copper [1] and its growth on metallic substrates have been the topic of several studies [2–6]. Thus, no previous study deeply elaborated the electrocrystallisation of copper on these three substrates.

In the first part, nucleation overpotentials were evidenced by cyclic voltammetry. Chronoamperometry studies were performed, and the experimental results were compared to theoretical plot to determine nucleation mode: instantaneous or progressive [7,8]. Afterwards, the germination rates were determined and the strategy (electrochemical parameters) for copper electrodeposition was deduced in order to increase the specific surface area of the electrode.

In the second part, the obtained bimetallic electrodes were employed to detect species requiring high sensitivity identification tools, such as nitrates in seawater. In the open ocean, the concentration of nitrates can drop from 50 µmol L^{-1} to as little as few nanomolars [9]. Surface waters are very depleted in nitrates (< 10 µmol L^{-1}).

The conventional method used to detect nitrates is colorimetry based on the Griess reaction requiring the addition of liquid reagents [10-11]. Lab on ship technology allows the miniaturization of the sensor and consequently decreases the volume of the reagent but these sensors still need frequent intervention to change reagents bags limiting long term deployment [12-13]. There is also commercial UV-absorbance nitrate sensor: SUNA that directly measure the concentration without pre-treatment [14]. However, interference issues with bromide ions, carbonates and dissolved organic matter are encountered and the limit of detection is 2.4 µmol L^{-1}. Electrochemistry is suitable for *in situ* applications because it does not require pre-treatment of the sample, offers a fast response time, high selectivity and allows small sizes sensor design and low energy consumption.

Various approaches have been pursued to study nitrate electroreduction with a large number of metal substrates, such as Pd, Pt, Rh, Ru, Ir, Cd, Pb, Ag, Ti, Au, Sn, Ni, Zn, alloys of Cu….[15–22]. The use of metallic bare electrodes for direct nitrates detection displayed weak sensitivity [23]. Few studies have demonstrated that nitrate electroreduction is more efficient on bimetallic electrodes [23-27], as the signal is boosted due to the increase of the specific surface area of the electrode.

Fajerwerg *et al.* [23] have already operated gold modified with silver nanoparticles electrode (Au/AgNPs) to detect nitrate in sodium chloride solution, using a charge, Q, lower than the theoretical one corresponding to a silver monolayer, and demonstrated the worthwhile potential of bimetallic electrode use. However, the limit of detection (LOD) of 10 µmol L^{-1} obtained was still too high for marine application. Later, Legrand *et al.* studied the influence

of the cutoff charge for silver electrodeposition on gold over the electrode sensitivity and reached a LOD of 0.39 µmol L^{-1} of nitrate in sodium chloride solution [27]. However, some repeatability issues were encountered.

The aim of this article is to highlight the necessity of controlling the electrodeposition process and optimizing the operation conditions in order to increase the sensitivity of the electrode.

As reported by several studies, copper is recognized as the best promoter for nitrate electroreduction in comparison with other metals. It was applied as a bare electrode given its resistance to biofouling [18,28,29], and accordingly, was chosen as the electrodeposited metal.

Since gold has previously been demonstrated to be a promising and noble substrate, it was used as a base for the bimetallic electrode.

In order to compare the electroactivity of Au/Cu modified electrode, platinum (Pt) was tested as a comparator substrate due to its similar properties. Stainless steel 316L (SS) was also considered for test alongside gold and platinum due to its low cost compared to the other metals used, as well as its known resistance to corrosion in seawater.

2. Experimental

2.1 Chemicals

All solutions were prepared in MilliQ water (Millipore MilliQ water system).

Nitrate solutions were prepared with KNO_3 (Aldrich 99.999%), dissolved into artificial seawater (pH=8) made with NaCl (m= 32.74 g L^{-1}, VWR), $NaHCO_3$ (m= 0.172 g L^{-1}, VWR) and $MgSO_4$, $7H_2O$ (m=7.26 g L^{-1}, VWR).

Copper electrodepositions on gold, stainless steel 316L and platinum surfaces were generated using 0.1 mol L^{-1} of copper sulfate pentahydrate $CuSO_4$, $5H_2O$ (99.995% purity) from Aldrich dissolved in 1 mol L^{-1} of sulfuric acid prepared from a 98% H_2SO_4 EMSURE® (Merck).

2.2- Materials and methods

Electrochemical techniques used were Chronoamperometry, Cyclic Voltammetry and Square Wave Voltammetry. Full electrochemical measurements were carried out with a Metrohm Autolab® PGSTAT 128N potentiostat controlled by NOVA 2.1.4 software.

A standard three electrodes cell was employed for all experiments. In all cases, the auxiliary electrode was a platinum wire with large surface area and the reference electrode was a double junction Ag/AgCl/KCl 3M electrode; all the following potentials are given relative to this electrode. Working electrodes were commercial metallic discs (ϕ= 6mm) of gold, platinum and stainless steel 316L (from Goodfellow) modified with copper electrodeposition.

The characterization of copper nuclei deposited on the substrate surface after electrolysis was observed by a Phenom XL scanning electron microscope (SEM) coupled with an energy dispersive spectroscopy (EDS).

2.3 Preparation of working electrodes

The substrate discs underwent an adapted polishing on metallographic polisher (Presi Mécapol), associated with diamond suspension solutions with different granulometries 9 µm, 3 µm and 1 µm. The duration of polishing on each grain size depends on the initial surface status.

For gold discs, a further electro-polishing was performed in sulfuric acid at 0.5 mol L^{-1} by polarizing the electrode 10 seconds at +2 V vs (Ag/AgCl/KCl) followed by 10 seconds at -2 V

vs (Ag/AgCl/KCl) to form O_2 and H_2 bubbles respectively. This leads to the removal of all impurities at the surface. Then cycles between 0 V vs (Ag/AgCl/KCl) and 1.5 V vs (Ag/AgCl/KCl) at 100 $mV.s^{-1}$ were recorded until reproducible signals were obtained.

3. Results and discussion

3.1 Determination of nucleation overpotentials

Cyclic voltammograms were plotted on gold, stainless steel, and platinum electrodes in a deaerated copper sulfate solution. Figure 1. shows the corresponding voltammograms obtained on gold (A), platinum (B) and stainless steel 316L (C) substrates.

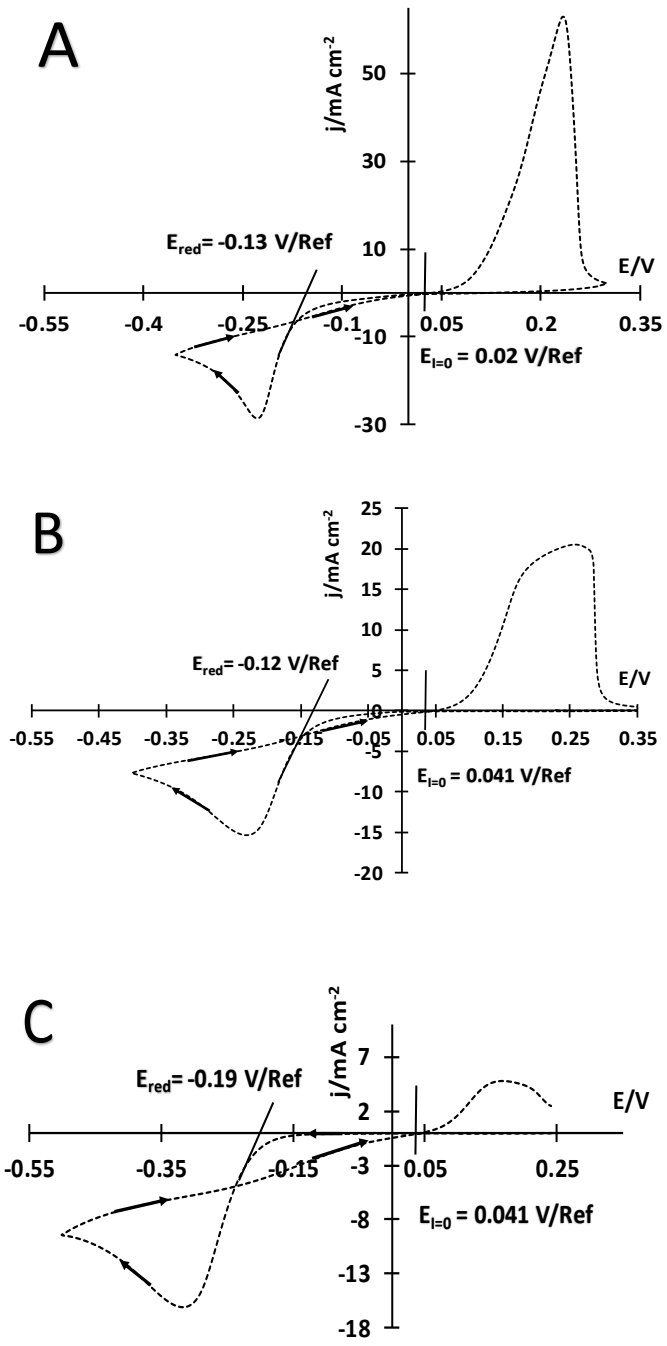

Figure 1. Cyclic voltammograms of $CuSO_4$ deaerated; working electrode: Pt (A), Au (B) and SS 316L (C); auxiliary electrode: Pt; reference electrode: Ag/AgCl/KCl; Scan rate = 50 mV s^{-1}

A single reduction peak was identified at around -0.2 V vs (Ag/AgCl/KCl) (for gold and platinum substrates), -0.3 V vs (Ag/AgCl/KCl) (for stainless steel) associated with a

reoxidation peak at around +0.2V vs (Ag/AgCl/KCl), +0.15 V vs (Ag/AgCl/KCl) respectively, characteristic of the dissolution of the deposited copper. Copper ions reduction in aqueous media was found to be a single step process exchanging 2 electrons:

$$Cu^{2+} + 2e^{-} \rightarrow Cu \ \#(1)$$

These voltammograms highlight the main feature of the electrocrystallisation process which is the signal crossing between forward and backward scanning curves (crossover). This is typical of a solid phase creation via nucleation mechanism on the electrode surfaces.

Furthermore, those voltammograms display nucleation overpotential corresponding to the difference between the potential of the beginning of the copper ion reduction E_{red} indicated with vertical lines on Figure 1. (first copper nuclei) and the equilibrium potential $E_{(I=0)}$ of Cu^{2+}/Cu system indicated with tangent lines:

$$\eta = E_{red} - E_{(I=0)} \#(2)$$

Where, ɳ corresponds to the nucleation overpotential, E_{red} the nuclei formation potential and $E_{(I=0)}$ the equilibrium potential. Nucleation overpotential values on three electrodes are presented in Table 1.

Electrode	Overpotential (mV)	10^4 AN_0 (cm^{-2} s^{-1})	Cutoff charge density (mC cm^{-2})	10^3 (Slope)
Pt/Cu	150	2.53	-51.8	9.61
Au/Cu	161	3.25	-23.5	3.91
SS 316L/Cu	231	3. 85	-16.58	1.02

Table 1. Overpotential, nucleation rate, cutoff charge density and slope on three substrates

These nucleation overpotential values are key parameters for electrodeposition because they represent the minimal requisite overpotentials during electrolysis.

3.2 Nucleation mode determination

Chronoamperometry is the most suitable electrochemical technique to investigate nucleation phenomena [7,8]. The exploitation of the beginning of the graphs I = f(t) provides information on the nucleation mode and, thus, enables the selection of a convenient process for the deposit. Chronoamperograms were recorded on the three substrates in copper sulfate solution and are presented on Figure 2.

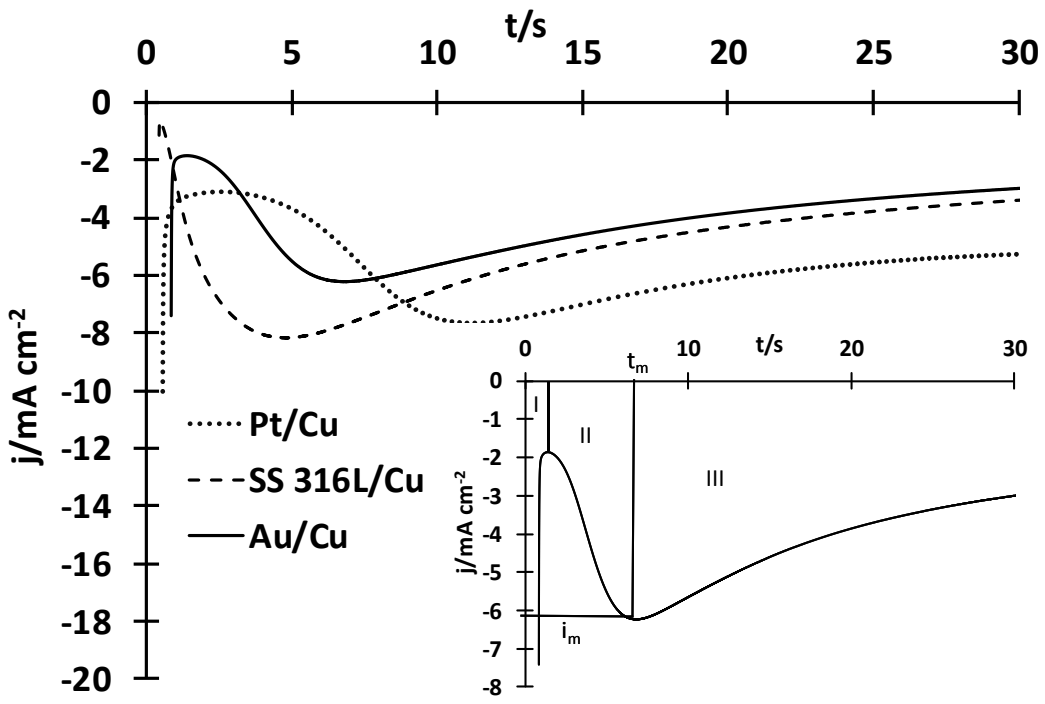

Figure 2. Chronoamperograms on Pt, Au, SS 316L electrode at η=150 mV, 160 mV, 231 mV, respectively in $CuSO_4$ solution at 0.1 mol L^{-1}. Auxiliary electrode: Pt; reference electrode: Ag/AgCl/KCl Inset: zoom of chronoamperogram on gold electrode η=150 mV

Numerous overpotentials were tested, and the electrochemical responses showed a good repeatability.

The resultant curves are divided into three parts; the inset of Figure 2 illustrates those three parts as follows:

- Part I is characterized by a significant decrease of current density, corresponding to the charge of the double layer and the formation of the first copper nuclei on the electrode surface.
- Part II of the chronoamperogram shows a current density increase, as a result of an upsurge of the electrode active surface. This zone represents a particular point at t_m, i_m coordinated where the rate of diffusion is equivalent to the rate of crystal growth. An investigation into part II of the chronoamperogram provides information on the nucleation mode.
- Part III shows a diminution in current density attributed to a limitation of the reaction by the diffusion phenomenon of copper ions Cu^{2+}, according to Cottrell's law: $I = f(t^{1/2})$ [30].

In order to identify the copper nucleation mode, Scharifker and Hills established a model based on a non-dimensional intensity and time: $(I/I_m)^2 = f(t/t_m)$ [7]. The mathematical model considers part II and part III of the chronoamperograms defining the two nucleation modes:

i) instantaneous nucleation where all the copper nuclei are generated at the same moment at the beginning of the polarization;

ii) progressive nucleation where new copper nuclei are continuously generated throughout the polarization.

The number of nuclei created versus time is given by the following equation [7,8]:

$$N = N_0\left(1 - e^{-(At)}\right) \#(3)$$

where N_o is the total number of favorable sites, A is the nucleation constant for a given site, t is time and N is the nuclei density.

For instantaneous nucleation, N = N_0 and the current density at the surface of the electrode is given by the expression [7,8]:

$$i = \frac{nFD^{\frac{1}{2}}C_0}{(\pi t)^{\frac{1}{2}}}\left\{1 - \exp{(-N\pi kDt)\#\#\#\#}\right\} \#(4)$$

Where n is the exchanged electrons number, F is the Faraday constant = 96500 C, D is the diffusion coefficient in $m^2\ s^{-1}$ and C_0 is the initial concentration in mol L^{-1},

With,

$$k = \left(\frac{8\pi C_0 M}{\rho}\right)^{0.5} \#(5)$$

M and ρ are the molar weight in g mol^{-1} and the specific mass in g L^{-1} , respectively, of copper.

However, for progressive nucleation, N = AN_0t, where AN_0 represents the germination rate. The following equation expresses the current density at the surface of the electrode:

$$i = \frac{nFD^{\frac{1}{2}}C_0}{(\pi t)^{\frac{1}{2}}}\left\{\frac{1 - \exp(-AN_0\pi k'Dt^2)\}}{2}\right\}\#(6)$$

Where;

$$k' = \frac{4}{3}\left(\frac{8\pi C_0 M}{\rho}\right)\#(7)$$

Expressions of I_m and t_m can be deduced by deriving equations 4 and 6 Gunawardena *et al.* [8] transformed these equations by integrating I_m and t_m. The following nondimensional equations are obtained:

i) for instantaneous nucleation

$$\left(\frac{I}{I_m}\right)^2 = \frac{1.9542}{\frac{t}{tm}}\left\{1-\exp\left[-1.2564\left(\frac{t}{tm}\right)\right]\right\}^2 \#(8)$$

Where;

$$t_m = \frac{1.2564}{N\pi kD} \#(9)$$

$$I_m = 0.6382nFDC_0(kN)^{0.5} \#(10)$$

And

$$I_m^2 t_m = 0.1629(nFC_0)^2 D \#(11)$$

ii) for progressive nucleation

$$\left(\frac{I}{I_m}\right)^2 = \frac{1.2254}{\frac{t}{tm}}\left\{1-\exp\left[-2.3367\left(\frac{t}{tm}\right)^2\right]\right\}^2 \#(12)$$

Where;

$$t_m = \left(\frac{4.6733}{AN_0\pi k'D}\right)^{0.5} \#(13)$$

$$I_m = 0.461nFD^{\frac{3}{4}}C_0(k'AN_0)^{0.25} \#(14)$$

And

$$I_m^2 t_m = 0.2598(nFC_0)^2 D \#(15)$$

Figure 3 shows experimental curves (j j_m^{-1}) ^{2}=f (t t_m^{-1}) plotted using chronoamperograms data obtained on Figure 2, compared to the theoretical curves calculated from equation 8 and equation 12.

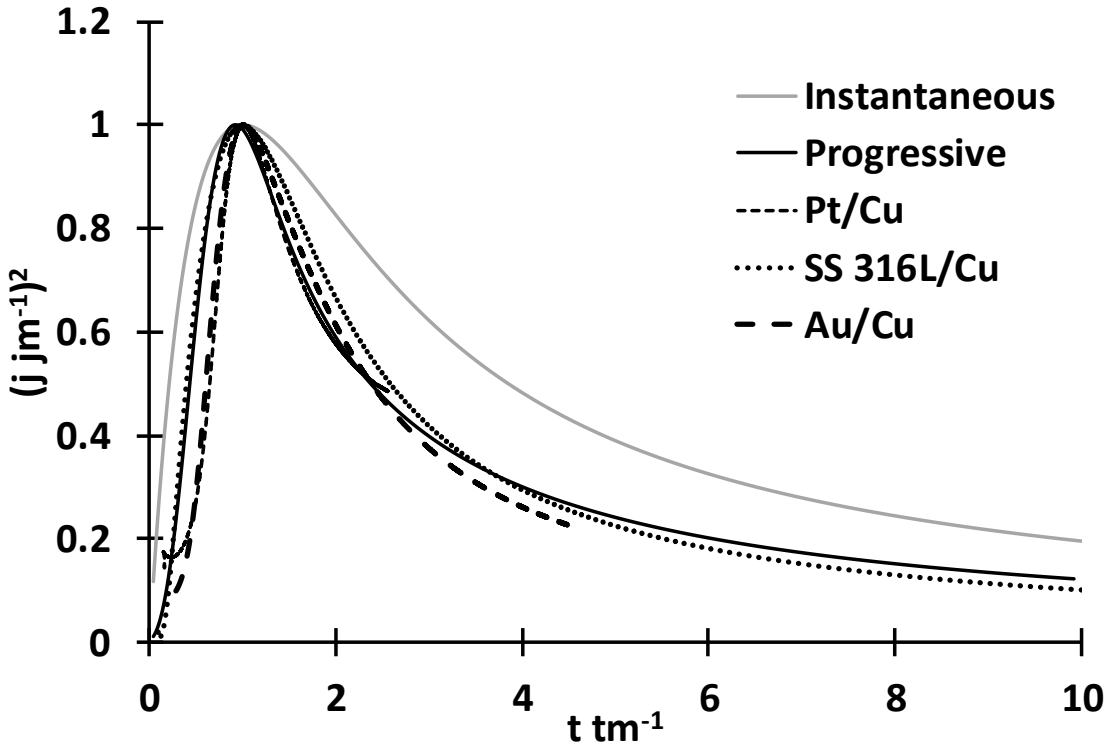

Figure 3. Comparison of the dimensionless experimental data obtained for the current - time transients on different metals calculated from Figure 2 with the theoretical model for instantaneous and progressive nucleation. Working electrodes: Pt, Au and SS 316L; auxiliary electrode: Pt; reference electrode Ag/AgCl/KCl

The experimental data are in agreement with equation 12 for a large t/t_m range proving that the nucleation of copper is progressive, whatever the substrate. Indeed, the geometry of the copper nuclei on the three substrates observed via scanning electron microscopy (SEM) on Figure 4 shows different sizes of copper particles characteristic of progressive nucleation mode in agreement with experimental results.

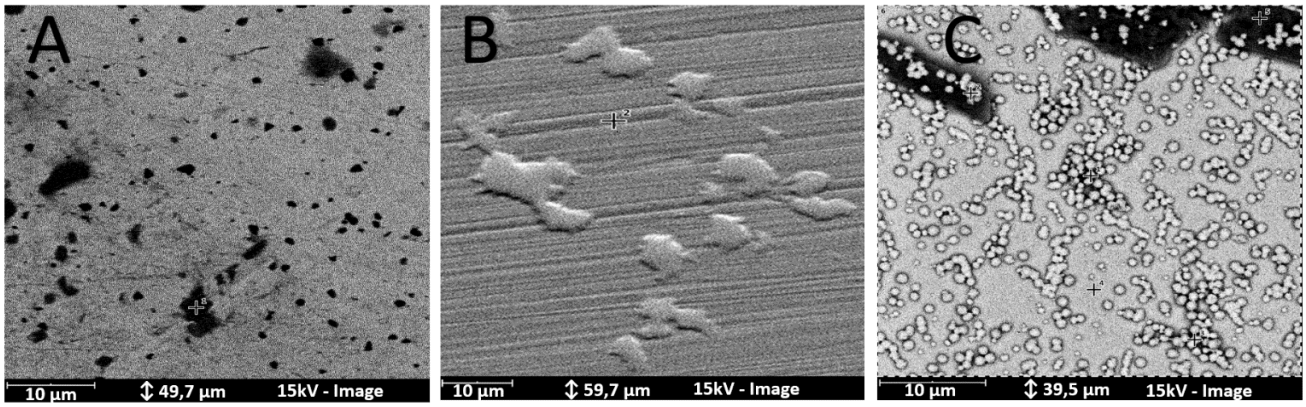

Figure 4 Scanning electron micrographs of copper nuclei on gold (A), platinum (B) and stainless steel 316L (C) electrodes

The hemispherical form of the copper nuclei was spotted. Besides their uneven sizes signifying that they were not generated at once, they are randomly distributed on the metallic surfaces. This observation confirms the consistency of copper's progressive nucleation on platinum, gold and stainless steel 316L.

This nucleation mode leads to the formation of new copper nuclei during the whole time of electrolysis. Each nuclei formed, then grew with time.

So the overall growth of the nuclei is controlled by two different rates:

(i) The germination rate is the number of nuclei generated versus time. The continuous formation of plots leads to a uniform distribution of the electrodeposited metal onto the surface of the electrode.

(ii) The growth rate represents how the size of the nuclei increases with time.

In our case it is mandatory to find a compromise between germination and growth rate aiming to generate heterogeneous small copper particles before covering the entire surface with deposited metal. Massot *et al.* suggested a relation between overpotential and roughness of the electrode [31]. Basically, effects (i) and (ii) are preponderant at:

- Low overpotentials due to the deposition of small metal particles on the substrate,
- And high overpotentials due to the heterogeneous distribution of the deposited metal on the layer formed after filling all available sites.

At intermediate values the roughness is considered satisfactory.

Based on this correlation, in order to obtain the largest bimetallic areas, it is necessary to impose the minimal overpotentials while stirring the solution to renew the diffusion layer and avoid the limitation by diffusion.

3.3 Determination of the nucleation rate AN_0

When the nucleation is progressive, it is possible to calculate the nucleation rate AN_0 after a short duration of electrolysis applying equations 13 and 14 where the value of copper ions' diffusion coefficient at 298.15 K was found around 8 10^{-6} cm^2 s^{-1}. Table 1 reports a difference between copper's nucleation rate on platinum, gold and stainless steel, interpreting that the substrate's nature influences the growth of electrodeposition.

3.4 Validation of the cutoff charge

As mentioned earlier, the optimization of the bimetallic electrode parameter such as cutoff charge and overpotential has an established impact on increasing electrode sensitivity. Hence, in order to improve the electrocatalytic properties of the electrode, it is crucial to control the exact quantity of copper particles deposited on the substrate surface and to, consequently, increase the active surface area.

As previously demonstrated, crystal growth in part II of chronoamperograms (Figure 2) is linked to an increase of the active surface area up to the maximum point at I_m and t_m before the diminution that results from the limitation by diffusion of copper ions. Therefore, the area under the curve in Figure 2. between t_0 and t_m yields the optimum theoretical cutoff charge to

apply during electrolysis to prepare the deposit of copper on different metals according to Faraday's law:

$$Q = \int_{o}^{tm} I.dt \ \#(16)$$

The optimum theoretical cutoff charge density found was |q|= 23.5 mC cm^{-2}.

In order to validate the cutoff charge, several charges were compared by detecting nitrate with SWV. The theoretically calculated charge was confirmed experimentally on the SWV presented in Figure 5. recorded with different cutoff charges in 1 mmol L^{-1} of nitrate in artificial seawater.

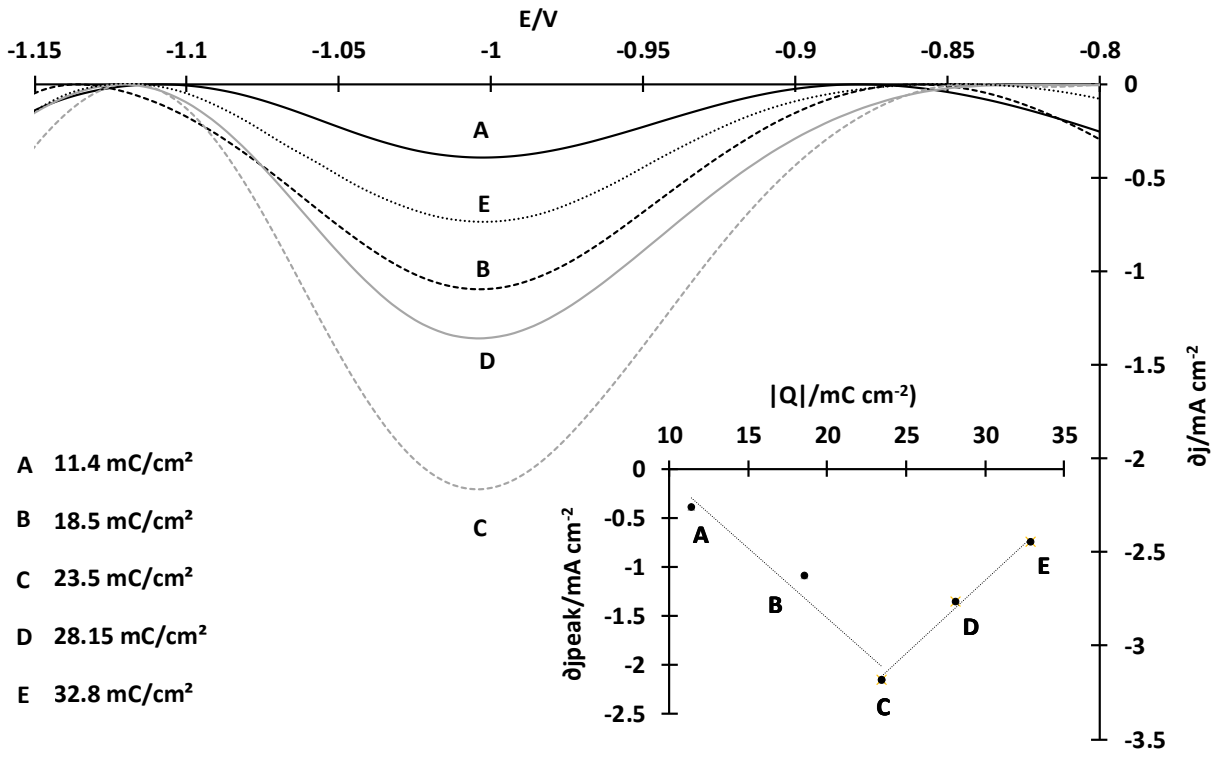

Figure 5. Square wave voltammograms obtained in 1 mmol L^{-1} of nitrates in artificial seawater illustrating the influence of cutoff charge density used for copper deposition on gold electrode Working electrodes: Au, auxiliary electrode: Pt; reference electrode: Ag/AgCl/KCl. Inset: corresponding to the Volcano plot $j_{peak}(NO_3^-) = f(|q|)$.

To obtain reproducible signals, SWV parameters were enhanced in terms of frequency, amplitude, and step potential. Theoretically, amplitude and step potential values are respectively $E_{sw} = 50/\eta$ and $E_{step} = 10/\eta$, where n is the number of exchanged electron(s) [31]. Considering the reduction of nitrate in nitrite with the following reaction:

$$NO_3^- + 2H^+ + 2e^- \leftrightarrow NO_2^- + H_2O \ \#(17)$$

Two electrons are exchanged, so E_{sw} should be around 25 mV and E_{step} around 5 mV. The signal frequency which enabled both sufficient sensitivity and minimal noise, was found to be between 25 Hz and 100 Hz.

The current density matching nitrate reduction around E = -1 vs (Ag/AgCl/KCl)/V on these voltammograms increases when the copper electrodeposition charge density increases from |q|= 11.4 mC cm^{-2} to 23.5 mC cm^{-2} as the effective surface area rises. However, increasing to 28.15 mC cm^{-2} and 32.8 mC cm^{-2} results in a drop in the nitrates reduction signal.

According to the Sabatier principle, when the activity of materials (cutoff charges in this case) are plotted versus the reactivity (peak intensity), the best condition is determined on a peak-shaped known as Volcano plot, corresponding to the intersection of the two straight lines (j_{peak} = |q|) in the inset of Figure 5 [32,33].

This behavior was observed previously by Legrand *et al.* [27]. This is due to the excessive growth of copper nuclei on the surface up to the point of coating the gold surface entirely, thus, the electrode behaves like a bare copper electrode.

The cutoff charge optimization was performed for other substrates. The optimum conditions to form modified electrodes are gathered in Table 1. These parameters were used to generate modified electrodes in order to proceed further in terms of direct detection of nitrate in artificial seawater, by SWV.

3.5 Nitrate detection using optimized bimetallic electrodes

SWV were recorded on Au/Cu, Pt/Cu and SS 316L/Cu electrodes in artificial seawater with different concentrations between 0.5 and 15 µmol L^{-1}. The peak intensities were measured at nearby -1 V vs (Ag/AgCl/KCl) corresponding to the concentration of nitrate reduction and the calibration curves presented on Figure 6.

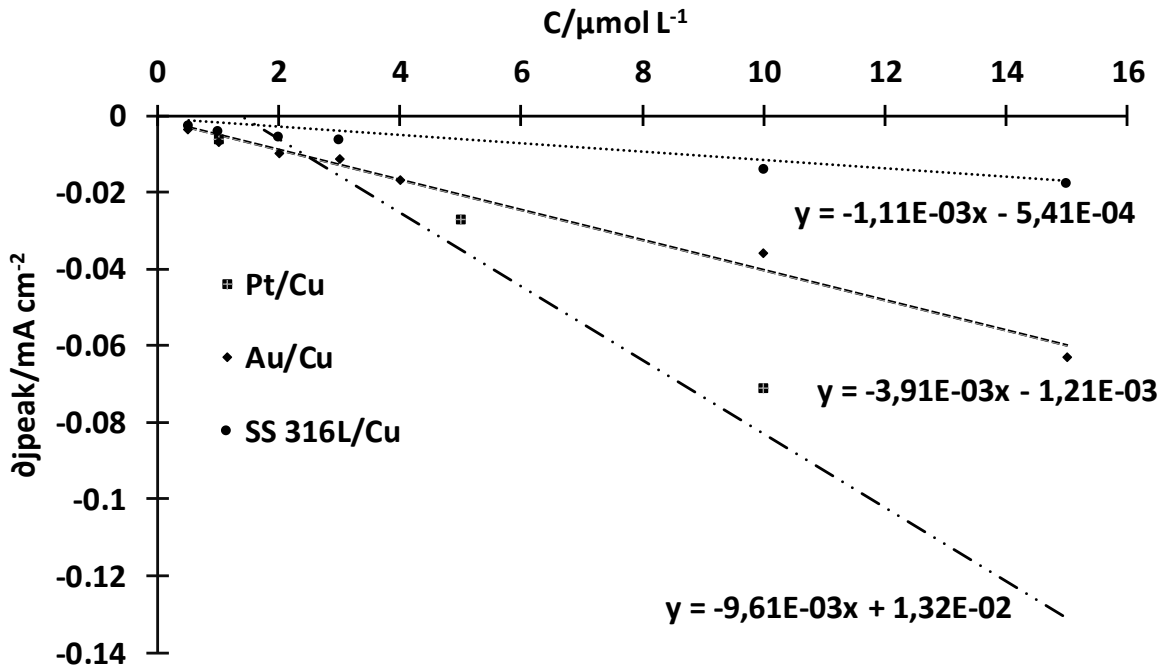

Figure 6. Calibration curves ipeak=([NO_3^-]) on Pt/Cu, Au/Cu and SS 16L/Cu for nitrates reduction peak around -1 V vs (Ag/AgCl/KCl) from SWV recorded between 0.5 and 15 µmol L^{-1} of nitrate in artificial seawater

Each electrode shows a linear behavior with nitrate concentration allowing to monitor nitrate in seawater while LOD, non-optimized yet, of 0.5 µmol L^{-1} is very promising.

The slopes are different on the three bimetallic electrodes; the modified electrode Pt/Cu shows an optimal slope, and thus better sensitivity than both Au/Cu and SS 316L/Cu. These results are in line with overpotential nucleation rate and cutoff charge density values as showed in Table 1 showing that the nucleation rate increases with the overpotential, while the cutoff charge density and the sensitivity (the slopes) are inv

ersely proportional. The following observations can be done: imposing a low overpotential signifies a low applied energy, so the nuclei production rate is slower, consequently higher duration is needed to reach the optimum bimetallic surface, and so, the cutoff charge is higher. And based on the aforementioned correlation suggested by Massot *et al.* [34] between overpotential and roughness, at lower overpotentials, the roughness should be higher due to the presence of two metals, so the sensitivity of the electrode is increased.

4. Conclusions

Our work focused on determining the best operating conditions to optimize the sensitivity of bimetallic electrodes. The electrocrystallisation of copper on platinum, gold and stainless steel 316L was investigated using cyclic voltammetry and chronoamperometry and led to the following conclusions:

- On the three substrates copper nuclei are generated progressively during electrolysis and the nucleation mode was confirmed by SEM analysis: hemispherical shape and uneven sizes were observed;
- Copper germination rate is higher on platinum than on gold and stainless steel 316L, respectively;

Optimum theoretical cutoff charges density for copper electrodeposition on the three substrates were calculated from the area under the curves j=f(t) between t_0 and t_m and were experimentally confirmed using a volcano plot where the best condition is determined on the peak of the diagram. Then these charges were applied to fabricate bimetallic electrodes with the highest active surface area.

In the second part, these modified electrodes were used to detect species demanding high sensitivity materials such as nitrate ions in seawater. the electroreduction of nitrate is not considerably different on various electrodes structures. Except the higher sensitivity on Pt/Cu

than on Au/Cu and on SS 316L/Cu. Finally, linear calibration curves were obtained for the nitrate concentration range tested (0.5 µmol L^{-1} – 15 µmol L^{-1}).

Acknowledgments

This work is supported by the Région Occitanie (ALDOCT-000781 / 19008749) and NKE Instrumentation based in Hennebont, France.

References

[1] D. Grujicic, B. Pesic, Electrodeposition of copper: the nucleation mechanisms, Electrochim. Acta. 47 (2002) 2901-2912. https://doi.org/10.1016/S0013-4686(02)00161-5

[2] P. M. Rigano, C. Mayer, T. Chierchie, Electrochemical nucleation and growth of copper on polycrystalline palladium, J. electro. chem. interfacial electrochem. 248 (1988) 219‑ 228. https://doi.org/10.1016/0022-0728(88)85163-5

[3] C. Ji, G. Oskam, P. C. Searson, Electrochemical nucleation and growth of copper on Si (111), Surf. Sci. 492 (2001) 115‑ 124. https://doi.org/10.1016/S0039-6028(01)01410-8

[4] G. Gunawardena, G. Hills, I. Montenegro, Electrochemical nucleation: Part IV. Electrodeposition of copper onto vitreous carbon, J. electro. chem. interfacial electrochem. 184 (1985) 357‑ 369. https://doi.org/10.1016/0368-1874(85)85539-8

[5] A. I. Danilov, E. B. Molodkina, Y. M. Polukarov, Initial stages of copper electrocrystallization from sulfate electrolytes: Cyclic voltammetry on a platinum ring-disk electrode, Russ. J. Electrochem. 36 (2000) 987–997. https://doi.org/10.1007/BF02757512

[6] G. Oksam, P.M Vereecken, P.C Searson, Electrochemical deposition of copper on n-Si/TiN, J. Electrochem. Soc. 146 (1999) 1436-1441. https://doi.org/10.1149/1.1391782

[7] B. Scharifker, G. Hills, Theoretical and experimental studies of multiple nucleation, Electrochim. Acta. 28 (1983) 879‑ 889. https://doi.org/10.1016/0013-4686(83)85163-9

[8] G. Gunawardena, G. Hills, I. Montenegro, B. Scharifker, Electrochemical nucleation: Part I. General considerations, J. electro. chem. interfacial electrochem. 138 (1982) 225‑ 239. https://doi.org/10.1016/0022-0728(82)85080-8

[9] S. Levitus, M. E. Conkright, J. L. Reid, R. G. Najjar, A. Mantyla, Distribution of nitrate, phosphate and silicate in the world oceans, Prog. Oceanogr. 31 (1993) 245‐ 273. https://doi.org/10.1016/0079-6611(93)90003-V

[10] M.D. Patey, M.J.A. Rijkenberg, P.J. Satham, M.C. Stinchcombe, E.P Achterberg, M. Mowlen, Determination of nitrate and phosphate in seawater at nanomolar concentrations, Trends Anal. Chem. 27 (2008) 169-182. https://doi.org/10.1016/j.trac.2007.12.006

[11] M. J. Moorcroft, J. Davis, R. G. Compton, Detection and determination of nitrate and nitrite: a review, Talanta. 54 (2001) 785‐ 803. https://doi.org/10.1016/S0039-9140(01)00323-X

[12] A.D. Beaton, C. Cardwell, R.S. Thomas, V.J. Sieben, F.E. Legrit, E.M Waugh, P.J Statham, M.C. Mowlem, H. Morgan, Lab-On-Chip measurement of nitrate and nitrite for *in situ* analysis of natural waters, Environ. Sci. 46 (2012) 9548-9556. https://doi.org/10.1021/es300419u

[13] A.D. Beaton, A.M. Schaap, R. Pascal, R.Hanz, U.Martincic, C.L. Cardwell, A. Morris, G. Clinton-Bailey, K. Saw, S. E. Hartman, M.C. Mowlem, Lab-on-Chip for *in situ* analysis of nutrients in the seep sea, ACS Sens. 7 (2022) 89-98. https://doi.org/10.1021/acssensors.1c01685

[14] G. MacIntyre, B. Plache, M. R. Lewis, J. Andrea, S. Feener, S. D. McLean, K. S. Johnson, L. J. Coletti, H. W. Jannasch, ISUS/SUNA nitrate measurements in networked ocean observing systems, OCEANS, (2009) 1-7. https://doi.org/10.23919/OCEANS.2009.5422251

[15] N. G. Carpenter, D. Pletcher, Amperometric method for the determination of nitrate in water, Anal. Chim. Acta. 317 (1995) 287‐ 293. https://doi.org/10.1016/0003-2670(95)00384-3

[16] I. Ul-Haque, M. Tariq, Electrochemical reduction of nitrate: a review, J. Che. Soc. Pak. 32 (2010) 396- 418.

[17] G. E. Dima, A. C. A. De Vooys, M. T. M. Koper, Electrocatalytic reduction of nitrate at low concentration on coinage and transition-metal electrodes in acid solutions, J. Electroanal. Chem. 554 (2003) 15- 23. https://doi.org/10.1016/S0022-0728(02)01443-2

[18] D. Pletcher, Z. Poorabedi, The reduction of nitrate at a copper cathode in aqueous acid, Electrochim. Acta. 24 (1979) 1253- 1256. https://doi.org/10.1016/0013-4686(79)87081-4

[19] M. Shibata, K. Yoshida, N. Furuya, Electrochemical synthesis of urea on reduction of carbon dioxide with nitrate and nitrite ions using Cu-loaded gas-diffusion electrode, J. Electroanal. Chem. 387 (1995) 143- 145. https://doi.org/10.1016/0022-0728(95)03992-P

[20] S. Cattarin, Electrochemical reduction of nitrogen oxyanions in 1 M sodium hydroxide solutions at silver, copper and CuInSe 2 electrodes, J. Appl. Electrochem. 22,(1992) 1077- 1081. https://doi.org/10.1007/BF01029588

[21] J. D. Genders, D. Hartsough, D. T. Hobbs, Electrochemical reduction of nitrates and nitrites in alkaline nuclear waste solutions, J. Appl. Electrochem. 26 (1996) 1- 9. https://doi.org/10.1007/BF00248182

[22] H.-L. Li, J. Q. Chambers, D. T. Hobbs, Electroreduction of nitrate ions in concentrated sodium hydroxide solutions at lead, zinc, nickel and phthalocyanine-modified electrodes, J. Appl. Electrochem. 18 (1988) 454- 458. https://doi.org/10.1007/BF01093762

[23] K. Fajerwerg, V. Ynam, B. Chaudret, V. Garçon, D. Thouron, M. Comtat, An original nitrate sensor based on silver nanoparticles electrodeposited on a gold electrode, Electrochem. Commun. 12 (2010) 1439- 1441. https://doi.org/10.1016/j.elecom.2010.08.003

[24] J. Davis, M. J. Moorcroft, S. J. Wilkins, R. G. Compton, M. F. Cardosi, Electrochemical detection of nitrate and nitrite at a copper modified electrode, Analyst. 125 (2000) 737‑ 742. http://dx.doi.org/10.1039/A909762G

[25] U. Prüsse, K.-D. Vorlop, Supported bimetallic palladium catalysts for water-phase nitrate reduction, J. Mol. Catal. A Chem. 173 (2001) 313‑ 328. https://doi.org/10.1016/S1381-1169(01)00156-X

[26] J. Liang, Y. Zheng, Z. Liu, Nanowire-based Cu electrode as electrochemical sensor for detection of nitrate in water, Sens. Actuators B: Chem. 232 (2016) 336‑ 344. https://doi.org/10.1016/j.snb.2016.03.145

[27] D. Chen Legrand, C. Barus, V. Garçon, Square Wave Voltammetry Measurements of Low Concentrations of Nitrate Using Au/AgNPs Electrode in Chloride Solutions, Electroanalysis. 29 (2017) 2282-2287. https://doi.org/10.1002/elan.201700447

[28] N. Aouina, H.Cachet, C.Debiemme-chouvy, T.Thi Tuyet Mai, Insight into the electroreduction of nitrate ions at a copper electrode, in neutral solution, after determination of their diffusion coefficient by electrochemical impedance spectroscopy, Electrochim. Acta. 55 (2010) 7341-7345. https://doi.org/10.1016/j.electacta.2010.07.032

[29] K. Rajeshwar, J. G. Ibanez, Environmental electrochemistry : Fundamentals and applications in pollution abatement. San Diego, 1997.

[30] A. J. Bard, L. R. Faulkner, J. L. Brisset, Electrochimie : principes, méthodes et applications. Masson, Paris, 1983.

[31] A. J. Bard, L. R. Faulkner, Fundamentals and applications, Electrochemical methods, second ed., John Wiley & sons, 2001.

[32] F. Calle-Vallejo, M. Huang, J. B. Henry, M. T. M. Koper, A.S. Bandarenka, Theoretical design and experimental implementation of Ag/Au electrodes for the electrochemical reduction of nitrate, Phys. Chem. Chem. Phys. 15 (2013) 3196‑ 3202. https://doi.org/10.1039/C2CP44620K

[33] A.B. Laursen, A.S Varela, F.Dionigi, H. Fanchiu, C. Miller, O.L Trinhammer, J.Rossmeisl, S. Dahl, Electrochemical Hydrogen Evolution: Sabatier's Principle and the Volcano Plot, J. Chem. Educ. 89 (2012) 1595-1599. https://doi.org/10.1021/ed200818t

[34] L. Massot, P. Chamelot, P. Palau, P. Taxil, Electrocrystallisation of tantalum in molten fluoride media, Electrochim. 50 (2005) 5408‑ 5413. https://doi.org/10.1016/j.electacta.2005.03.021